



# A review of homogenization and topology optimization III—topology optimization using optimality criteria

B. Hassani, E. Hinton \*

*Department of Civil Engineering, University of Wales, Swansea, Singleton Park, Swansea, SA2 8PP, U.K.*

Received 28 January 1997; accepted 28 April 1998

---

## Abstract

This is the third part of a three paper review of homogenization and topology optimization. In the first two papers the homogenization theory and solution of the equations for different material models to be used in topology optimization by the homogenization method are described. In this paper, the mathematical model for the topological structural optimization is constructed and derivation of the related optimality criteria is explained. A modified resizing scheme is suggested. Finally, in explaining the employed algorithm some illustrative examples are provided. © 1998 Elsevier Science Ltd. All rights reserved.

---

## 1. Introduction

In Part II of these review papers, by introducing different material models, we noticed how the complex nature of the structural topology (or layout) optimization problem can be changed to an easier sizing problem. The design variables of the optimization problem are the geometrical parameters defining the microstructures of the assumed composite material in each finite element.

To solve the topology optimization problem any non-linear mathematical programming method may be used. These methods are usually robust and can be applied to any sort of optimization problem. However, when applied to structural optimization problems, several calculations of the objective function, constraint functions and their derivatives (i.e. several structural and sensitivity analyses) are usually needed [1,2]. Because of this, the required computer time for mathematical programming methods is largely dependent on the number of design variables, which means that

when the number of design variables increases, these methods become very costly and time consuming [3].

In structural topology, optimization based on the homogenization concept, the number of design variables is proportional to the number of elements of the discretized domain. Consequently, the use of mathematical programming methods for realistic topology optimization problems is somewhat impractical, as they usually require hundreds of finite elements, and therefore hundreds of design variables. To overcome this deficiency “optimality criteria” methods have been considered.

Optimality criteria methods were developed in the late 1960s as an alternative approach to mathematical programming methods for solving structural optimization problems. The fundamental ideas behind optimality criteria methods were originally introduced by Michell in 1904 [4]. An excellent review of the history of optimality criteria methods is given in Chapter 9 of a book by Rozvany [5].

The optimality criteria methods are indirect methods of optimization, unlike mathematical programming methods which directly optimize the objective function. Optimality criteria methods attempt to satisfy a set of criteria related to the behaviour of the structure. These

---

\* Corresponding author.

criteria are derived either intuitively or rigorously. “Fully stressed design” and “simultaneous failure mode design” are examples of intuitive optimality criteria methods. Rigorously derived optimality criteria methods, often based on Kuhn–Tucker optimality conditions, are used in the algorithm developed in PLATO and are therefore the subject of this chapter.

Optimality criteria methods for structural optimization have been used by two groups of researchers: the so-called analytical and numerical schools [6, 7]. The newly developed, discretized, continuum-type optimality criteria technique (DCOC) [8, 7] takes advantage of the approaches adopted in both schools and is more useful than continuum-based optimality criteria (COC) methods [7, 9].

The continuum-based optimality criteria (COC) are usually derived by variational methods. Rozvany and his coworkers [5, 6, 10] reinterpret the derived optimality criteria as equilibrium, compatibility and generalized strain–stress relations for a fictitious system called the *adjoint structure*. This fictitious structure is used as a convenient mechanical analogy for interpreting certain quantities in optimality criteria. This interpretation has two advantages. First, engineers can visualize it more easily than an abstracted mathematical problem and second, the analysis of the adjoint structure, as well as the actual structure, can be carried out with the finite element method [10].

In iterative COC methods applied to discretized problems, each iteration consists of two basic steps: first, the analysis of the real and adjoint systems and second, the update of the design variables [10].

The rapidly increasing computational capacity of modern computers and the necessity for discretization in most practical problems have provided the main motives for DCOC methods. In the DCOC method developed by Rozvany and his coworkers, the general optimality criteria for discretized structural systems are derived on the basis of the flexibility formulation of matrix analysis and the Kuhn–Tucker optimality conditions. An iterative algorithm for coupling the DCOC method with finite element analysis is then developed [9].

Optimality criteria methods are especially efficient for problems with large numbers of design variables and few constraints. These criteria are, in fact, necessary (and sometimes sufficient) conditions for minimality of the objective function.

Although closed form analytical solutions can be achieved for very limited and idealized systems, they

are very important in checking the validity and applicability of numerical methods as well as discovering the fundamental features of optimal solutions. Hence, in the following, two simple illustrative examples will be presented.

## 2. Kuhn–Tucker Optimality Conditions

The optimization problem in its general form can be expressed as follows:

$$\begin{aligned} &\text{Minimize } f(x) \\ &\text{such that } h_j(x) = 0, \quad j = 1, 2, \dots, n_h; \\ &\quad g_k(x) \leq 0, \quad k = 1, 2, \dots, n_g \end{aligned} \quad (1)$$

where  $x = (x_1, x_2, \dots, x_n)$  are design variables and  $n_h$  and  $n_g$  are, respectively, the number of equality and inequality constraints.

Using the Kuhn–Tucker conditions [11], we can establish a test to be applied to a candidate point to see whether that point is a minimum or not, instead of solving the set of nonlinear equations. For convex minimization problems<sup>1</sup>, the necessary Kuhn–Tucker conditions, are also sufficient. Furthermore, any local minimum is a global one.

The necessary Kuhn–Tucker optimality conditions for the optimization problem in its general form of Eq. (1) can be written as

$$\begin{aligned} &\frac{\partial f}{\partial x_i} + \sum_{j=1}^{n_h} \lambda_j \frac{\partial h_j}{\partial x_i} + \sum_{k=1}^{n_g} v_k \frac{\partial g_k}{\partial x_i} = 0 \quad i = 1, \dots, n, \\ &h_j = 0 \quad j = 1, \dots, n_h, \\ &g_k \leq 0 \quad k = 1, \dots, n_g, \\ &g_k v_k = 0 \quad k = 1, \dots, n_g, \\ &v_k \geq 0 \quad k = 1, \dots, n_g \end{aligned} \quad (2)$$

where  $\lambda_j$  and  $v_k$  are Lagrangian multipliers. It is important to note that by changing the optimization problem from finding a minimum to a maximum, or by changing the sign of constraint terms in the Lagrangian, or by changing the direction of the inequality constraints, each time, the sign of multipliers  $v_k$  in the Kuhn–Tucker conditions (Eq. (2)) will change [12].

## 3. Analytical Optimality Criteria

As mentioned in the introduction, analytical optimality criteria (OC) methods, apart from having an important role in the development of OC methods, are used for the verification of numerical algorithms. In this section, two illustrative examples are considered. Our objective in the first example is to give a concise introduction to the variational method and terminology

<sup>1</sup> If the objective function and feasible domain of a problem are convex, it is called a *convex programming* problem. Convexity of the feasible domain occurs if all the inequality constraints are convex and the equality constraints are linear.

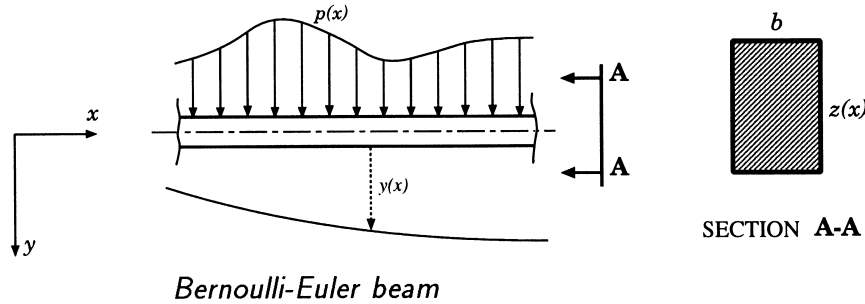


Fig. 1. Bernoulli–Euler beam.

frequently used by the analytical school [5]. The object of the second example is first, to explain the main aspects of the procedure of the analytical method and second, we will use the results for verification of the algorithm developed in this review. We hope that this will help engineers engaged with numerical techniques to have better communication with the analytical school.

### 3.1. An illustrative example of variational analysis

As a simple example of the derivation of the analytical optimality criteria for a continuum structure, the Bernoulli–Euler beam problem, with a single criterion is considered here [13]. The height of the cross section  $z(x)$  and the deflection of the beam  $y(x)$  are assumed to be, respectively, the design variable and response (state) functions. (See Fig. 1). Note that the admissible functions  $y$  should satisfy the kinematic boundary conditions. The objective function is given in the form of a global measure as  $\int_0^L \rho(x)y(x)dx$ , where  $\rho(x)$  is a specified weighting on the beam displacement  $y(x)$ . The lower bound for  $z$  and the upper bound for the volume of the beam are, respectively, denoted by  $z^0$  and  $V$ . The state (equilibrium) equation of the beam is

$$\frac{d^2}{dx^2} \left( EI(x) \frac{d^2 y(x)}{dx^2} \right) - p(x) = 0 \quad (3)$$

(and boundary conditions).

<sup>2</sup> This can be verified by noticing that the objective function is, in fact, the external work done by the virtual force  $\rho(x)$  on the real displacements  $y(x)$  on the real displacements  $y(x)$ , which is equal to the internal work, that is

$$\Phi = \int_0^L \rho y dx = \int_0^L \frac{M \bar{M}}{S} dx = \int_0^L S \bar{y}'' y'' dx$$

where  $M = Sy''$  and  $\bar{M} = S\bar{y}''$  are the moments of inertia and differentiating it results in

$$\frac{d\Phi}{dz} = \frac{dS}{dz} \bar{y}'' y''.$$

Consequently, the optimal problem design may be constructed as

$$\begin{aligned} & \text{Minimize} \quad \int_0^L \rho(x)y(x)dx \\ & \text{subject to} \quad (S(x, z(x))y''(x))'' - p(x) = 0, \\ & \quad \quad \quad z^0 - z(x) \leq 0, \\ & \quad \quad \quad \int_0^L bz(x)dx - V \leq 0 \end{aligned} \quad (4)$$

where  $L$  is the length of the beam,  $S$  is the bending rigidity ( $EI$ ) and where a superscript (') implies differentiation with respect to  $x$ . By using Kuhn–Tucker conditions as explained in the last section, the Lagrangian of Eq. (4) may be written as

$$\begin{aligned} \mathcal{L} = & \int_0^L \rho(x)y(x)dx + \int_0^L \bar{y}(x)[(S[x, z(x)]y'')'' - p(x)]dx \\ & + \int_0^L \gamma(x)[z^0 - z(x)]dx + \Gamma \left[ \int_0^L bz(x)dx - V \right], \end{aligned} \quad (5)$$

where  $y(x)$ ,  $\gamma(x)$  and  $\Gamma$  are Lagrange multipliers. From stationarity of  $\mathcal{L}$  with respect to  $y$  and by cancelling the terms with opposite signs in the related Euler–Lagrange equation [or equivalently by four times integration by parts from the second term of Eq. (5)], it follows that

$$\{S[x, z(x)]\bar{y}''(x)\}'' - \rho(x) = 0. \quad (6)$$

This equation is very similar to the state Eq. (3) and the only difference is the loading. Because of this similarity it is called an *adjoint system*. Similarly, stationarity of  $\mathcal{L}$  with respect to  $z(x)$  results in

$$\frac{dS(x, z)}{dz} \bar{y}'' + \gamma(x) - \Gamma b = 0. \quad (7)$$

This equation is referred to as the *optimality criterion*. The term  $dS/dz \bar{y}'' y''$  is, in fact, the *gradient* of the objective function with respect to the design variable  $z(x)^2$ . Using the Kuhn–Tucker conditions, the other optimality conditions are obtained; that is

$$z^0 - z(x) \leq 0; \quad \gamma(x)[z^0 - z(x)] = 0; \quad \gamma(x) \geq 0 \quad (8)$$

and

$$\int_0^L bz(x)dx - V \leq 0; \quad \Gamma \left[ \int_0^L bz(x)dx - V \right] = 0; \quad \Gamma \geq 0. \quad (9)$$

$dS/dz\bar{y}''y''$  is also the *specific mutual energy* between the original and *adjoint* states. We note that over intervals where  $z(x) > z^0$ , according to Eq. (8)  $\gamma(x) = 0$ . Thus, the optimality condition requires that the gradient of the objective function, or the specific mutual energy, has to be of constant value. This is the optimality criteria.

If the weighting function  $\rho(x)$  in the preceding example equals the primary load [i.e.  $\rho(x) = p(x)$ ], then the solutions of Eqs. (3) and (6) are the same, so that  $y(x) = \bar{y}(x)$ . This implies that the adjoint structure in terminology used by Rozvany [5, 6, 10]) is the same as the real structure. Also we note that, in this case, the objective function is a measure of *compliance*.

### 3.2. An illustrative example of derivation of optimality criteria

The problem of exact layout optimization of a plane truss with the objective of minimizing the weight of the structure and subject to several load conditions and displacement constraints is addressed by Rozvany and coworkers [6, 8]. Here the problem of minimum compliance (maximum stiffness) with an upper side volume constraint and single load case is considered. We will see that the optimality criteria are the same and the result obtained will be used as a benchmark to check the numerical algorithm developed.

Following Rozvany et al [6], we first derive the optimality criteria for a finite number of truss elements with lower side constraints for the cross sectional area of elements. The mathematical expression of the problem may be written as

$$\begin{aligned} &\text{Minimize} \quad \frac{1}{2} \mathbf{p}^T \mathbf{u} \\ &\text{subject to} \quad \frac{1}{2} \mathbf{p}^T \mathbf{u} = \frac{1}{2} \sum_{i=1}^n \frac{f_i^2 l_i}{a_i E_i}, \\ &\quad a_i^0 - a_i \leq 0, \quad i = 1, \dots, n; \\ &\quad \sum_{i=1}^n a_i l_i - V \leq 0 \end{aligned} \quad (10)$$

where  $\mathbf{p}$  and  $\mathbf{u}$  are, respectively, the external load and the related displacement vectors.  $n$  is the number of elements,  $f_i$  is the internal force in element  $i$  and  $a_i$ ,  $l_i$  and  $E_i$  are, respectively, the cross-sectional area, length and modulus of elasticity of member  $i$  of the truss.

The symbol  $V$  stands for the volume and  $a_i^0$  is the lower bound of the cross-sectional area. The optimization problem (Eq. (10)) can also be simplified as

$$\begin{aligned} &\text{Minimize} \quad \sum_{i=1}^n \frac{f_i^2 l_i}{a_i E_i} \\ &\text{subject to} \quad a_i^0 l_i - a_i l_i \leq 0 \quad i = 1, \dots, n; \\ &\quad \sum_{i=1}^n a_i l_i - V \leq 0. \end{aligned} \quad (11)$$

The Lagrange function may be constructed as

$$\mathcal{L} = \sum_{i=1}^n \frac{f_i^2 l_i}{a_i E_i} + \sum_{i=1}^n \lambda_i (a_i^0 l_i - a_i l_i) + \Gamma \left( \sum_{i=1}^n a_i l_i - V \right), \quad (12)$$

where  $\lambda_i$  and  $\Gamma$  are the Lagrange multipliers. Employing the Kuhn–Tucker conditions it follows that

$$-\frac{f_i^2 l_i}{a_i^2 E_i} - \lambda_i l_i + \Gamma l_i = 0, \quad i = 1, 2, \dots, n; \quad (13)$$

$$\lambda_i \geq 0; \quad \lambda_i (a_i^0 - a_i) = 0, \quad i = 1, 2, \dots, n; \quad (14)$$

$$\Gamma \geq 0; \quad \Gamma \left( \sum_{i=1}^n a_i l_i - V \right) = 0. \quad (15)$$

It is important to note that in this problem  $\Gamma$  in Eqs. (13)–(15) can not be zero and it is a strictly positive number. This can be proved by considering Eq. (13) where assuming  $\Gamma = 0$  results in

$$\frac{f_i^2 l_i}{a_i E_i} = -\lambda_i a_i l_i. \quad (16)$$

According to Eq. (14)  $\lambda_i \geq 0$  and it can be concluded that

$$\frac{1}{2} \frac{f_i^2 l_i}{a_i E_i} \leq 0. \quad (17)$$

But the left hand side of Eq. (17) is the strain energy of element  $i$  of the truss which can not be negative or zero (which implies infinite rigidity), which is not possible. The cross sectional area can be obtained from Eq. (13) as

$$a_i = \sqrt{\frac{f_i^2}{(\Gamma - \lambda_i) E_i}}. \quad (18)$$

Therefore, from the switching conditions (14) it follows that

$$\begin{aligned} &\text{if } a_i > a_i^0 \quad \text{then } \lambda = 0 \quad \text{and} \quad a_i = \sqrt{\frac{f_i^2}{\Gamma E_i}}, \\ &\text{if } a_i = a_i^0 \quad \text{then } \lambda = 0 \quad \text{and} \quad a_i \leq \sqrt{\frac{f_i^2}{\Gamma E_i}}. \end{aligned} \quad (19)$$

Using the definition of strain  $\epsilon = f_i/a_i E_i$  and substituting into Eq. (19) results in

$$\begin{cases} \sqrt{\frac{E_i}{\Gamma}} \epsilon_i = 1 & \text{for } a_i > a_i^0, \\ \sqrt{\frac{E_i}{\Gamma}} \epsilon_i \leq 1 & \text{for } a_i = a_i^0. \end{cases} \quad (20)$$

If we define a *criterion function*  $\Phi$  as

$$\Phi = \sqrt{\frac{E_i}{\Gamma}} \epsilon_i \quad (21a)$$

then Eq. (20) can be reduced to

$$\begin{cases} \Phi = 1 & \text{for } a_i > a_i^0, \\ \Phi \leq 1 & \text{for } a_i = a_i^0. \end{cases} \quad (21b)$$

Now, we extend the derived criteria to vanishing cross-sections by letting  $a_i \rightarrow 0$  (note that  $\Gamma$  is still greater than zero because  $\Gamma = 0$  leads us to a truss with infinite rigidity), Eq. (21b) can be written as

$$\begin{cases} \Phi = 1 & \text{for } a_i > 0, \\ \Phi \leq 1 & \text{for } a_i = 0. \end{cases} \quad (22)$$

Now, we are in the position to extend the result obtained to the “structural universe” with an infinite number of elements, i.e. to a continuum media comprising an infinite number of truss-like elements in all potential directions. In this case, at each point  $(x, y)$  of the domain of interest a potential truss member passing through that point, can be represented by the coordinates of the point and the orientation  $\theta$  of the member. Therefore, the strain in each member ( $\epsilon_i$ ) can well be identified by  $\epsilon(x, y, \theta)$ . Hence, Eq. (22) in this case is changed to

$$\begin{aligned} \Phi(x, y, \theta) &= 1 & \text{for } a(x, y, \theta) > 0, \\ \Phi(x, y, \theta) &\leq 1 & \text{for } a(x, y, \theta) = 0. \end{aligned} \quad (23)$$

So far, we have come to the conclusion that the optimality criteria for the problem of a minimum weight truss with some constraints on the displacements and stresses (which has been addressed by many researchers) and the problem of minimum compliance with a side constraint on the volume (or weight) are identical. The only difference is that in the latter, the real and adjoint structure (see Ref. 6) are the same.

Now, following a procedure similar to the one introduced by Rozvany et al [6], we argue that  $\Phi = \epsilon(x, y, \theta) \sqrt{E_i/\Gamma}$  has a maximum value in the direction of non-vanishing (here this implies optimal) members. Thus, at each point  $(x, y)$  there exists an optimal passing member in the direction  $\theta^*$  only if

$$|\epsilon(x, y, \theta^*)| = \max_{\theta} |\epsilon(x, y, \theta)| \quad (24)$$

where  $\theta^*$  is a specific value of  $\theta$ .

It is interesting to notice that the “continuum universe” of the problem can equivalently be thought of as a two (or three) dimensional elasticity problem. Consequently, for a kinematically admissible displacement field, the direction of the maximum principal strain at each point matches the direction of the optimal member. Furthermore, from Eq. (21a) it is observed that the optimality criteria function is proportional to the strain. Therefore, by normalizing our problem (i.e. adopting  $\sqrt{E/\Gamma} = 1$  which does not affect the optimum layout), we can conclude that the condition for optimal members is  $|\epsilon_1| = 1$ . We note that the direction of the minor principal strain is orthogonal to the direction of the major principal strain and in general  $|\epsilon_2| \leq 1$ .

Now, let us consider the problem of a single vertical load in Fig. 2 which is to be optimally transmitted to a vertical support. The kinematic boundary conditions are

$$u(0, y) = v(0, y) = 0 \quad (25)$$

where  $u$  and  $v$  are displacements in the  $x$  and  $y$  directions, respectively. Therefore, the optimal layout can be defined as a set of points which belong to the half plane  $\{(x, y) | x \geq 0\}$  that satisfy Eq. (25) and the optimality criteria  $|\epsilon_1| = 1$ . Following Rozvany et al [6, 8], the displacement field

$$u(x, y) = 0 \quad \text{and} \quad v(x, y) = 2x \quad (26)$$

satisfies Eq. (25) and leads to

$$\begin{aligned} \epsilon_x &= du/dx = 0, & \epsilon_y &= dv/dy = 0, \\ \gamma_{xy} &= du/dy + dv/dx = 2 \end{aligned} \quad (27)$$

which results in

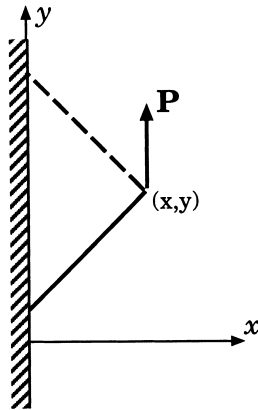
$$\epsilon_1 = 1, \quad \epsilon_2 = -1 \quad \text{and} \quad \alpha = \pm 45^\circ \quad (28)$$

where  $\alpha$  is the direction of principal strains. The result obtained implies that the optimal bars must run at  $\pm 45^\circ$  to the vertical and must be in tension and compression, respectively, in the two principal directions. By removing the potential members with zero forces, the two bar truss of Fig. 2 is the optimum layout.

#### 4. Mathematical Model for the Topological Structural Optimization Problem

Let us consider the general linear elasticity problem subject to the applied body force  $\mathbf{f}$  in a bounded open domain  $\Omega$  and the surface traction forces  $\mathbf{t}$  on  $\Gamma_t$ . Assume that  $\Omega$  has a smooth boundary  $\Gamma$  comprising  $\Gamma_d$ , where displacements are prescribed and  $\Gamma_t$ , where traction forces are applied. It is also assumed that

$$\Gamma_t \cup \Gamma_d = \Gamma \quad \text{and} \quad \Gamma_t \cap \Gamma_d = \emptyset. \quad (29)$$



Optimal layout

Fig. 2. Optimal layout.

As described in Section 6 of the Part I paper, by applying the virtual displacement method, the equilibrium equation can be obtained by equating the external and internal virtual works. Assuming  $\mathbf{u}$  to be the displacement field that defines equilibrium of the elastic structure and  $\mathbf{v}$  to be the kinematically admissible virtual displacement field, so that

$$\mathbf{v} \in \mathbf{V} \quad \text{where} \quad \mathbf{V} = \{\mathbf{v} | \mathbf{v} \in [H^1(\Omega)]^3 \quad \text{and} \quad \mathbf{v} = 0 \text{ on } \Gamma_d\}, \quad (30)$$

then for the elastic structure with a fixed boundary on  $\Gamma_d$  we have that

$$\int_{\Omega} \boldsymbol{\epsilon}^T(\mathbf{v}) [\mathbf{D}\boldsymbol{\epsilon}(\mathbf{u})] d\Omega = \int_{\Omega} \mathbf{f}^T \mathbf{v} d\Omega + \int_{\Gamma_t} \mathbf{t}^T \mathbf{v} d\Gamma. \quad (31)$$

By borrowing the notation from functional analysis and using the energy bilinear form for the internal work and the load linear form for external work [14, 15], Eq. (31) can be written as

$$a(u, v) = l(v), \quad \forall \mathbf{v} \in \mathbf{V} \quad (32)$$

where

$$a(u, v) = \int_{\Omega} \boldsymbol{\epsilon}(\mathbf{v}) \cdot [\mathbf{D}\boldsymbol{\epsilon}(\mathbf{u})] d\Omega \quad (33)$$

and

$$l(v) = \int_{\Omega} \mathbf{f} \cdot \mathbf{v} d\Omega + \int_{\Gamma_t} \mathbf{t} \cdot \mathbf{v} d\Gamma. \quad (34)$$

<sup>3</sup> According to the principal of minimum potential energy “among all the admissible displacement functions, the actual displacements make the total potential energy an absolute minimum [17]”.

The structural optimization problem in one of its most general forms aims to find the stiffest possible structure using a certain amount of material. A structure with maximum global stiffness provides a minimum value for the external work with the real displacement field or minimum *mean compliance*  $l(u)$ . Therefore, the structural optimization problem with the mean compliance as objective function can be constructed as,

$$\begin{aligned} &\text{Minimize} \quad l(u) \\ &\text{subject to} \quad a(u, v) = l(v) \quad \forall \mathbf{v} \in \mathbf{V} \\ &\quad \text{and} \quad \text{design restrictions} \end{aligned} \quad (35)$$

where design restrictions,  $a(u, v)$  and  $l(v)$  are functions of the design variables. As we have seen before, the design variables of the structural topology optimization problem are the geometrical parameters representing the microscale perforations of the presumed material model (e.g.  $a$ ,  $b$  and  $\theta$  in the material model comprising square cells with the rectangular holes and  $\gamma$ ,  $\mu$  and  $\theta$  for the rank-2 material).

If the structure is fixed on the boundary  $\Gamma_d$ , then by substituting  $\mathbf{u} \in \mathbf{V}$  instead of  $\mathbf{v}$  in Eq. (32) the following equation is obtained

$$a(u, u) = l(u). \quad (36)$$

Remembering that  $1/2a(u, u)$  is the strain energy, we observe that minimizing the mean compliance is equivalent to minimizing the strain energy.

On the other hand, the *total potential energy* can be written as

$$\Pi(u) = \frac{1}{2}a(u, u) - l(u) \quad (37)$$

and by substituting from Eq. (36) it follows that

$$\Pi(u) = -\frac{1}{2}l(u). \quad (38)$$

From Eq. (38) it is concluded that minimizing the mean compliance is equivalent to maximizing the total potential energy. Therefore, the optimization problem (Eq. (35)) can be written as:

$$\begin{aligned} &\text{Maximize} \quad \Pi(u) \\ &\text{subject to} \quad a(u, v) = l(v) \quad \forall \mathbf{v} \in \mathbf{V} \\ &\quad \text{and} \quad \text{design restrictions,} \end{aligned} \quad (39)$$

whereas, by using the principle of minimum potential energy<sup>3</sup> Eq. (39) can be written as

$$\begin{aligned} &\max_{\text{design}} \quad \min_{\mathbf{v} \in \mathbf{V}} \quad \Pi(\mathbf{v}), \\ &\text{subject to} \quad \text{design restrictions} \end{aligned} \quad (40)$$

Construction of the optimization problem based on the total potential energy is preferred, because it is more general and it always describes an optimization problem for the stiffest structure. While, in the case of prescribed boundary displacements, using the “mean compliance” or the “strain energy” as the objective function may lead to confusion [16]. This point can be realized by noticing the fact that in the case of having a non-zero prescribed displacement, and in the absence of body forces and tractions, the stiffest structure corresponds to the maximum strain energy (and maximum mean compliance), while in most of the cases the strain energy should be minimized.

In the general case of enforcing the prescribed boundary displacements  $\bar{\mathbf{u}}$  on  $\Gamma_d$ , by using the exterior penalty method [2,18] and applying a “sufficiently large” penalty coefficient  $\beta$ , the total potential energy will be formed as

$$\begin{aligned} \Pi_\beta(v) = & \int_{\Omega} \epsilon(v) \cdot \mathbf{D}\epsilon(u) d\Omega - \int_{\Omega} \mathbf{f} \cdot v d\Omega \\ & - \int_{\Gamma_t} \mathbf{t} \cdot v d\Gamma + \beta \int_{\Gamma_d} (v - \bar{\mathbf{u}})^2 d\Gamma. \end{aligned} \quad (41)$$

It is noted that minimizing  $\Pi_\beta(v)$  is equivalent to solving the equation of equilibrium and it yields the displacements  $\mathbf{u}$ .

If the material model with rectangular holes is used<sup>4</sup>, considering  $a$ ,  $b$  and  $\theta$  as distributed functions and recalling the relations of Section 2.1 of the part II paper, the optimization problem (40) can be expressed as

$$\begin{aligned} & \max_{a,b,\theta} \min_{v \in V} \Pi_\beta(v), \\ \text{subject to } & \Omega_s = \int_{\Omega} (1 - ab) d\Omega \leq \bar{\Omega}_s \\ & \text{and } 0 \leq a, b \leq 1. \end{aligned} \quad (42)$$

where  $\Omega_s$  is the upper limit on the volume of the solid material. Eq. (42) is equivalent to

$$\begin{aligned} & \max_{a,b,\theta} \Pi(u), \\ \text{subject to } & \Omega_s \leq \bar{\Omega}_s \\ & \text{and } 0 \leq a, b \leq 1. \end{aligned} \quad (43)$$

In the next section the optimality conditions for the adopted mathematical model Eq. (43), are derived.

## 5. Optimality Criteria for the Topological Structural Optimization Problem

### 5.1. Optimality conditions

By using the Lagrange multipliers and the Kuhn–Tucker conditions, the necessary conditions for optimality in Eq. (43) are obtained. Adopting the finite element method for the analysis, we assume that the design variables  $a$ ,  $b$  and  $\theta$ , as explained in Section 2.1 of the Part II paper, are constant parameters inside each finite element. Therefore, Eq. (43) for a discretized problem can be written as

$$\begin{aligned} & \text{Maximize} && \Pi(u) \\ & a^e, b^e, \theta^e && (e = 1, \dots, N) \\ \text{such that} &&& \sum_{e=1}^N (1 - a^e b^e) \Omega^e - \bar{\Omega}_s \leq 0, \\ & \text{and} && a^e - 1 \leq 0 \quad e = 1, \dots, N, \\ & && -a^e \leq 0 \quad e = 1, \dots, N, \\ & && b^e - 1 \leq 0 \quad e = 1, \dots, N, \\ & && -b^e \leq 0 \quad e = 1, \dots, N, \end{aligned} \quad (44)$$

where  $N$  is the number of elements and  $\Pi(u)$  in the discretized domain is

$$\begin{aligned} \Pi(u) = & \frac{1}{2} \sum_{e=1}^N \int_{\Omega^e} \epsilon^T(u) D^e \epsilon(u) d\Omega - \sum_{e=1}^N \int_{\Omega^e} \mathbf{u}^T \mathbf{f} d\Omega \\ & - \sum_{e=1}^N \int_{\Gamma_t^e} \mathbf{u}^T \mathbf{t} d\Gamma. \end{aligned} \quad (45)$$

Now, introducing multipliers  $\lambda_{a0}^e, \lambda_{a1}^e, \lambda_{b1}^e, (e = 1, \dots, N)$  and  $\Lambda$ , the Lagrangian function  $\mathcal{L}$  associated with Eq. (44) may be constructed as

$$\begin{aligned} \mathcal{L} = & \Pi(u) - \Lambda \left[ \sum_{e=1}^N (1 - a^e b^e) \Omega^e - \bar{\Omega}_s \right] \\ & - \sum_{e=1}^N \lambda_{a0}^e (-a^e) - \sum_{e=1}^N \lambda_{a1}^e (a^e - 1) \\ & - \sum_{e=1}^N \lambda_{b0}^e (-b^e) - \sum_{e=1}^N \lambda_{b1}^e (b^e - 1). \end{aligned} \quad (46)$$

Stationarity of  $\mathcal{L}$  with respect to  $a^e$  requires that

$$\frac{\partial \Pi(u)}{\partial a^e} + \Lambda b^e \Omega^e + \lambda_{a0}^e - \lambda_{a1}^e = 0, \quad (e = 1, \dots, N) \quad (47)$$

and by substituting for  $\Pi(u)$  from Eq. (45), it follows that

$$\begin{aligned} \frac{1}{2} \int_{\Omega^e} \epsilon^T(u) \frac{\partial \mathbf{D}^e}{\partial a^e} \epsilon(u) d\Omega - \int_{\Omega^e} \mathbf{u}^T \frac{\partial \mathbf{f}}{\partial a^e} d\Omega + \Lambda b^e \Omega^e + \lambda_{a1}^e = 0. \end{aligned} \quad (48)$$

<sup>4</sup> In the case of rank-2 material, because of the strong similarity, it is enough to replace  $a$  and  $b$  with  $\gamma$  and  $\mu$ .

Similarly, stationarity of  $\mathcal{L}$  with respect to  $b^e$  and  $\theta^e$  yield

$$\frac{1}{2} \int_{\Omega^e} \boldsymbol{\epsilon}^T(u) \frac{\partial \mathbf{D}^e}{\partial b^e} \boldsymbol{\epsilon}(u) d\Omega - \int_{\Omega^e} \mathbf{u}^T \frac{\partial \mathbf{f}}{\partial b^e} d\Omega + \Lambda a^e \Omega^e + \lambda_{b0}^e - \lambda_{b1}^e = 0 \quad (49)$$

and

$$\frac{1}{2} \int_{\Omega^e} \boldsymbol{\epsilon}^T(u) \frac{\partial \mathbf{D}^e}{\partial \theta^e} \boldsymbol{\epsilon}(u) d\Omega = 0, \quad (e = 1, \dots, N). \quad (50)$$

Now, using the Kuhn–Tucker conditions, similar to Eq. (2), the switching conditions are obtained as

$$\sum_{e=1}^N (1 - a^e b^e) \Omega^e - \bar{\Omega}_s \leq 0, \quad \Lambda \left[ \sum_{e=1}^N (1 - a^e b^e) \Omega^e - \bar{\Omega}_s \right] = 0, \quad \Lambda \geq 0, \quad (51)$$

$$a^e - 1 \leq 0, \quad \lambda_{a1}(a^e - 1) = 0, \quad \lambda_{a1} \geq 0, \quad e = 1, \dots, N; \quad (52)$$

$$-a^e \leq 0, \quad \lambda_{a0}(-a^e) = 0, \quad \lambda_{a0} \geq 0, \quad e = 1, \dots, N; \quad (53)$$

$$b^e - 1 \leq 0, \quad \lambda_{b1}(b^e - 1) = 0, \quad \lambda_{b1} \geq 0, \quad e = 1, \dots, N; \quad (54)$$

$$-b^e \leq 0, \quad \lambda_{b0}(-b^e) = 0, \quad \lambda_{b0} \geq 0, \quad e = 1, \dots, N. \quad (55)$$

The set of non-linear Eqs. (48)–(55) provide  $7N + 1$  equations ( $N$  is the number of finite elements) with the same number of unknowns to be solved.

The solution of these equations is a point of the design space which satisfies the necessary conditions of optimality. Since solving these equations is not an easy task, we try to establish an optimality criteria algorithm, instead. Based on these criteria, an updating scheme is constructed. By starting from a feasible point in the design space and using the scheme, at each iteration the design variables are updated so that we gradually move towards the optimum point. A method based on this concept has proved to be computationally very efficient, although it can not be

guaranteed that it will always converge to the global optimum.

## 5.2. Updating scheme

Employing the traditional optimality criteria method [19] an updating scheme for the design variables (e.g.  $a^e$ ,  $b^e$  and  $\theta^e$ ) can be constructed. To derive this scheme, the mutual influences of the design variables on each other, also from element to element, are ignored and in each iteration step they are updated independently.

Although the angle of rotation  $\theta^e$  can be updated inside the iteration scheme, in order to increase the convergence speed, following Bendsøe and Kikuchi [16, 18] and making use of the results of research done on optimal orientation of orthotropic material, we deal with it separately. Therefore, in the updating scheme the cell size parameters  $a$  and  $b$  ( $\gamma$  and  $\mu$  for rank-2 material) are resized. The issue of the optimal orientation is the subject of the next section.

If we define

$$E_a^e = \frac{\frac{1}{2} \int_{\Omega^e} \boldsymbol{\epsilon}^T(u) (\partial \mathbf{D}^e / \partial a^e) \boldsymbol{\epsilon}(u) d\Omega - \int_{\Omega^e} \mathbf{u}^T (\partial \mathbf{f} / \partial a^e) d\Omega}{-\Lambda b^e \Omega^e}, \quad (56)$$

then Eq. (48) can be written as

$$E_a^e = 1 + \frac{\lambda_{a0}^e}{\Lambda b^e \Omega^e} - \frac{\lambda_{a1}^e}{\Lambda b^e \Omega^e}. \quad (57)$$

It is noted that if we assume that the lower and upper side constraints for  $a^e$  are not active (i.e.  $0 < a^e < 1$ ), then  $\lambda_{a0}^e = \lambda_{a1}^e = 0$  and Eq. (57) becomes:  $E_a^e = 1$ .

Now, let us imagine that in iteration  $k$ , the design variable  $a_k^e$  has been decreased in order to move towards optimum point. Therefore,  $a_k^e < 1$  and the upper side limit is not active, which yields  $\lambda_{a1}^e = 0$ . Thus, noticing that  $\Lambda b^e \Omega^e$  is a positive real number and  $\lambda_{a0}^e \geq 0$ , from Eq. (57) it follows that  $E_a^e \leq 1$ . On the other hand, for increasing  $a_k^e$  we will get  $E_a^e \leq 1$ . So, inspired by this argument, we calculate the value of  $E_a^e$  and compare it with unity. If  $E_a^e > 1$ , then we let  $a_k^e$  decrease by the *move limit*  $\zeta$  [i.e.  $a_{k+1}^e = a_k^e(1 - \zeta)$ ] and if  $E_a^e < 1$ , then  $a_{k+1}^e = a_k^e(1 + \zeta)$ . Based on this conclusion and considering the side limits for  $a^e$  (i.e.  $0 \leq a^e \leq 1$ ), Bendsøe et al [16] have suggested the following resizing scheme:

$$a_{k+1}^e = \begin{cases} \min\{(1 + \zeta)a_k^e, 1\} & \text{if } a_k^e(E_a^e)_k \leq \max\{(1 - \zeta)a_k^e, 0\}, \\ a_k^e[(E_a^e)_k]^\eta & \text{if } \max\{(1 - \zeta)a_k^e, 0\} < a_k^e(E_a^e)_k < \min\{(1 + \zeta)a_k^e, 1\}, \\ \max\{(1 - \zeta)a_k^e, 0\} & \text{if } \min\{(1 + \zeta)a_k^e, 1\} \leq a_k^e(E_a^e)_k. \end{cases} \quad (58)$$



We now define

$$E_b^e = \frac{\frac{1}{2} \int_{\Omega^e} \epsilon^T(u) (\partial \mathbf{D}^e / \alpha b^e) \epsilon(u) d\Omega - \int_{\Omega^e} \mathbf{u}^T (\partial \mathbf{f} / \partial b^e) d\Omega}{-A d^e \Omega^e}. \quad (59)$$

Then,  $b^e$  can be updated as

$$b_{k+1}^e = \begin{cases} \min\{(1 + \zeta)b_k^e, 1\} & \text{if } b_k^e(E_b^e)_k \leq \max\{(1 - \zeta)b_k^e, 0\}, \\ b_k^e[(E_b^e)_k]^\eta & \text{if } (1 - \zeta)b_k^e, 0 < b_k^e(E_b^e)_k < \min\{1 + \zeta)b_k^e, 1\}, \\ \max\{(1 - \zeta)b_k^e, 0\} & \text{if } \min\{(1 + \zeta)b_k^e, 1\} \leq b_k^e(E_b^e)_k. \end{cases} \quad (60)$$

Here  $\eta$  is a damping factor and subscript  $k$  denotes the iteration number.

To have a monotonic algorithm, the approximate value of the damping factor  $\eta$  can be obtained by equating the resizing values for the switching points ( $E = 1 - \zeta$  and  $E = 1 + \zeta$ ) which leads to

$$(1 - \zeta)^\eta = 1 + \zeta \quad (61)$$

and

$$(1 + \zeta)^\eta = 1 - \zeta. \quad (62)$$

From Eqs. (61) and (62), respectively, it follows that

$$\eta = \frac{\ln(1 + \zeta)}{\ln(1 - \zeta)} \quad (63)$$

and

$$\eta = \frac{\ln(1 - \zeta)}{\ln(1 + \zeta)}. \quad (64)$$

Assuming  $\zeta$  to be a small value and using the Taylor series expansion, from both Eqs. (63) and (64) it follows that

$$\eta \simeq -1 + \zeta. \quad (65)$$

It is important to note that  $(E_a^e)_k$  and  $(E_b^e)_k$  depend on the current value of  $A_k$ , the Lagrange multiplier of the

active volume constraint, which needs to be adjusted in an inner iteration loop. For this purpose, the standard methods like the Newton–Raphson iterative procedure or the bisection method can be employed. As the Newton–Raphson method requires the extra computational effort of calculating  $d\Omega_s/dA$  (e.g. by the finite difference method), here the bisection method is

adopted. According to this procedure, and noting that  $d\Omega_s/dA < 0$ , the steps below are followed:

1. find  $A_{\min}^0$  and  $A_{\max}^0$  such that

$$\Omega_s(A_{\min}^0) > \bar{\Omega}_s \quad \text{and} \quad \Omega_s(A_{\max}^0) < \bar{\Omega}_s;$$

2. calculate

$$A^m = \frac{1}{2}(A_{\min}^m + A_{\max}^m);$$

3. calculate  $\Omega_s(A^m)$  and update either  $A_{\min}$  or  $A_{\max}$  as

$$\begin{aligned} \text{if } \Omega_s < \bar{\Omega}_s \quad \text{then } A_{\max}^{m+1} &= A^m, \\ \text{if } \Omega_s > \bar{\Omega}_s \quad \text{then } A_{\min}^{m+1} &= A^m; \end{aligned}$$

4. Increase the iteration number by one, and repeat steps 2 and 3 until  $|\Omega_s - \bar{\Omega}_s| \leq \delta$ .

Here,  $\delta$  indicates the acceptable tolerance for the volume constraint.

Note that for stability of the algorithm, the move size  $\zeta$  and the tolerance for the volume constraint  $\delta$  have to be adjusted. As a general rule, in order to have a larger move size  $\zeta$ , the volume constraint must be more relaxed.

### 5.3. A modified resizing scheme

In the resizing scheme which was described, it is noted that the difference between the values of the cell size parameters (design variables) in two successive iteration (e.g.  $a_k^e$  and  $a_{k+1}^e$ ) is proportional to the

magnitude of the parameters. This means that, while the larger values of  $a^e$  and  $b^e$  vary rapidly, the updating rates for small values are very small. In fact, an infinite number of iterations are needed to reach zero. It is also noted that use of conditional “if” commands in the scheme may affect the stability of the algorithm and they are better avoided.

In order to have a better monotonic and stable algorithm, by following the arguments similar to the last section, the following resizing scheme is suggested:

$$a_{k+1}^e = \begin{cases} \min \left\{ \left( 1 + \frac{\zeta}{|a_k^e - \zeta|} \right) a_k^e, 1 \right\} & \text{if } a_k^e (E_a^e)_k \leq \max\{(1 - \zeta)a_k^e, 0\}, \\ a_k^e [(E_a^e)_k]^{-\frac{1}{a_k^e}} & \text{if } \max\{(1 - \zeta)a_k^e, 0\} < a_k^e (E_a^e)_k < \min\{1 + \zeta, 1\}, \\ \max \left\{ \left( 1 - \frac{\zeta}{|a_k^e - \zeta|} \right) a_k^e, 0 \right\} & \text{if } \min\{(1 + \zeta)a_k^e, 1\} \leq a_k^e (E_a^e)_k \end{cases} \quad (66)$$

and

$$b_{k+1}^e = \begin{cases} \min \left\{ \left( 1 + \frac{\zeta}{|b_k^e - \zeta|} \right) b_k^e, 1 \right\} & \text{if } b_k^e (E_b^e)_k \leq \max\{(1 - \zeta)b_k^e, 0\}, \\ b_k^e [(E_b^e)_k]^{-\frac{1}{b_k^e}} & \text{if } \max\{(1 - \zeta)b_k^e, 0\} < b_k^e (E_b^e)_k < \min\{1 + \zeta, 1\}, \\ \max \left\{ \left( 1 - \frac{\zeta}{|b_k^e - \zeta|} \right) b_k^e, 0 \right\} & \text{if } \min\{(1 + \zeta)b_k^e, 1\} \leq b_k^e (E_b^e)_k. \end{cases} \quad (67)$$

With a similar move size  $\zeta$  this modified scheme is much faster than the former one.

## 6. Optimal Orientation

As was noted earlier, the design variables of the structural topology optimization problem consist of sizing variables ( $a^e$  and  $b^e$ ) and orientation variables ( $\theta^e$ ). In the last section, the resizing scheme for the size variables were considered. In this section, the issue of optimal values for the orientation variables are discussed. Having determined the sizing design variables  $a^e$  and  $b^e$  by the resizing scheme, the current problem is how to determine  $\theta^e$  to maximize (or minimize) the objective function.

By means of coordinate transformation formulae, we are able to relate the elasticity properties of the fixed system,  $\mathbf{D}^H(a^e, b^e)$ , and the rotated system,  $\mathbf{D}^G(a^e, b^e, \theta^e)$ . The general elasticity tensor  $E_{ijkl}^G$  can be computed by [20]

$$E_{ijkl}^G(a^e, b^e, \theta^e) = \sum_{p=1}^2 \sum_{q=1}^2 \sum_{r=1}^2 \sum_{s=1}^2 a_{ip}(\theta^e) a_{jq}(\theta^e) a_{kr}(\theta^e) a_{ls}(\theta^e) \times E_{pqrs}^H(a^e, b^e) \quad (68)$$

where in the case of 2-D problems, the rotation matrix is defined by

$$\mathbf{a}(\theta^e) = \begin{bmatrix} \cos \theta^e & -\sin \theta^e \\ \sin \theta^e & \cos \theta^e \end{bmatrix}. \quad (69)$$

Note that  $\mathbf{D}^G$  is the compact form of  $E_{ijkl}^G$ . We also note that the following relation may be used

$$\mathbf{D}^G(a^e, b^e, \theta^e) = \mathbf{R}^T(\theta^e) \mathbf{D}^H(a^e, b^e) \mathbf{R}(\theta^e), \quad (70)$$

where by equating the strain energy density of the fixed and rotated frames,  $\mathbf{R}(\theta^e)$  is obtained as

$$\mathbf{R}(\theta^e) = \begin{bmatrix} \cos^2 \theta^e & \sin^2 \theta^e & \cos \theta^e \sin \theta^e \\ \sin^2 \theta^e & \cos^2 \theta^e & -\cos \theta^e \sin \theta^e \\ -2 \cos \theta^e \sin \theta^e & 2 \cos \theta^e \sin \theta^e & \cos^2 \theta^e - \sin^2 \theta^e \end{bmatrix}. \quad (71)$$

Now, we consider the problem of how to update the design variables. Apart from mathematical programming methods, the following methods have been used by researchers to update the orientational design variable  $\theta^e$ :

1. principal strain method (Pederson's method);
2. principal stress method;
3. stress based optimality criteria method; and
4. strain based optimality criteria method.

### 6.1. Principal strain method

This method is based on Pederson's discussion [21] on the problem of optimal orientation of an orthotropic material in order to obtain an extreme strain energy density. Noting Eq. (36), the strain energy density is equal to one half of the mean compliance in a unit volume. In Pederson's problem, the elasticity matrix  $\mathbf{D}$  is fixed and a rotating strain field exists. Writing the strain energy density in terms of principal strains, he concluded that "material axes which are also principal strain axes always give stationary energy density" [21].

Cheng et al [22] have argued that this consideration does not fulfill the requirements of the real design problem and the results of this method are relatively poor. The discussion by Pederson is local and is limited to only a special point of the design domain. Hence, it is applicable to a unit cell case where the orientational design variable is separated from the whole design domain to obtain extreme strain energy density. In other words, instead of stationarity of the strain energy density, the strain energy corresponding to the whole design domain has to be considered.

In the topology design problem, the strain field and principal strains and their directions are dependent on the orientation variable and can change when the orientation variable  $\theta$  is varied. In fact, these changes can be caused not only by the variations of  $\theta$  at the considered point, but also the variations of the other spatial points of the design domain. Especially when the finite element discretization is used, the coupling will exist between the discrete orientation variables of the various finite elements. This method was suggested by Bendsøe [23] as an alternative to an iterative Newton type algorithm. "For materials with square microvoids, the cells should be rotated along the directions of principal strain" [23].

### 6.2. Principal stress method

The use of the principal stress directions as the optimal orientation was considered by Suzuki and Kikuchi [18]. The intuitive idea behind this is that, having a constant stress field with respect to the orientational variable, to obtain the stiffest structure, the principal material axis should be coalescent with the principal stress direction. This method, although lack-

ing a mathematical basis, provides quite good results (c.f. Ref. [22]).

Díaz and Bendsøe [24] extended this method for a multiple load case. In their approach, first the principal stress directions for different load cases are determined and then, by considering the obtained equation from stationary of the Lagrangian with respect to  $\theta^e$ , a combined equation is obtained. By solving this equation the optimal orientation is determined.

### 6.3. Strain based optimality criteria method

Following a similar procedure to the one proposed by Cheng et al, the sensitivity of  $\mathbf{D}(a^e, b^e, \theta^e)$  with respect to the orientational variable in element  $e$  can be written as

$$\frac{\partial \mathbf{D}^e}{\partial \theta^e} = \frac{\partial \mathbf{R}^T(\theta^e)}{\partial \theta^e} \mathbf{D}^H(a^e, b^e) \mathbf{R}(\theta^e) + \mathbf{R}^T(\theta^e) \mathbf{D}^H(a^e, b^e) \frac{\partial \mathbf{R}(\theta^e)}{\partial \theta^e}. \quad (72)$$

Substituting for  $\mathbf{R}(\theta^e)$  from Eq. (71) in Eq. (72) and applying Eq. (50) results in

$$\alpha_1^e \cos 2\theta^e - \alpha_2^e \sin 2\theta^e + \alpha_3^e \cos 4\theta^e - \alpha_4^e \sin 4\theta^e = 0, \quad (e = 1, \dots, N) \quad (73)$$

where

$$\alpha_1^e = \frac{1}{2} (D_{11}^H - D_{22}^H) \int_{\Omega^e} \epsilon_{12} (\epsilon_{11} + \epsilon_{22}) d\Omega, \quad (74a)$$

$$\alpha_2^e = \frac{1}{2} (D_{11}^H - D_{22}^H) \int_{\Omega^e} (\epsilon_{11}^2 - \epsilon_{22}^2) d\Omega, \quad (74b)$$

$$\alpha_3^e = \frac{1}{2} (D_{11}^H + D_{22}^H - 2D_{12}^H - 4D_{66}^H) \times \int_{\Omega^e} \epsilon_{12} (\epsilon_{11} - \epsilon_{22}) d\Omega, \quad (74c)$$

$$\alpha_4^e = \frac{1}{4} (D_{11}^H + D_{22}^H - 2D_{12}^H - 4D_{66}^H) \times \int_{\Omega^e} [(\epsilon_{11} - \epsilon_{22})^2 - \epsilon_{12}^2] d\Omega. \quad (74d)$$

We observe that in Eq. (73) are  $N$  nonlinear coupled equations which should be solved by iterative techniques. If we assume that the coefficients are not sensitive to the variations of the discretized orientational variable  $\theta^e$ , then Eq. (74) can be approximately solved for each individual element.

### 6.4. Stress based optimality criteria method

This procedure is very similar to the strain based method, but instead of strains, stresses are considered. Substituting  $\boldsymbol{\epsilon} = \mathbf{D}^{-1} \boldsymbol{\sigma} = \mathbf{C} \boldsymbol{\sigma}$  in Eq. (50) it yields

$$\int_{\Omega^e} \boldsymbol{\sigma}^T \frac{\partial \mathbf{C}^e}{\partial \theta^e} \boldsymbol{\sigma} d\Omega = 0, \quad (e = 1, \dots, N). \quad (75)$$

Following a procedure similar to the strain based method results in the equations below which are very similar to the strain based case:

$$\beta_1^e \cos 2\theta^e - \beta_2^e \sin 2\theta^e + \beta_3^e \cos 4\theta^e - \beta_4^e \sin 4\theta^e = 0, \quad (e = 1, \dots, N) \quad (76)$$

where

$$\beta_1^e = \frac{1}{2} (C_{11}^H - C_{22}^H) \int_{\Omega^e} \sigma_{12} (\sigma_{11} + \sigma_{22}) d\Omega, \quad (77a)$$

$$\beta_2^e = \frac{1}{2} (C_{11}^H - C_{22}^H) \int_{\Omega^e} (\sigma_{11}^2 - \sigma_{22}^2) d\Omega, \quad (77b)$$

$$\begin{aligned} \beta_3^e &= \frac{1}{2} (C_{11}^H + C_{22}^H - 2C_{12}^H - 4C_{66}^H) \\ &\times \int_{\Omega^e} \sigma_{12} (\sigma_{11} - \sigma_{22}) d\Omega, \end{aligned} \quad (77c)$$

$$\begin{aligned} \beta_4^e &= \frac{1}{4} (C_{11}^H + C_{22}^H - 2C_{12}^H - 4C_{66}^H) \\ &\times \int_{\Omega^e} [(\sigma_{11} - \sigma_{22})^2 - \sigma_{12}^2] d\Omega. \end{aligned} \quad (77d)$$

As with the last case, the set of expressions in Eq. (76) may be solved by iterative solution techniques.

Cheng et al [22] in their research have concluded that “strain response is much more sensitive than the stress response for both statically determinate and indeterminate structures and much stronger coupling exists among the orientational variables when the strain field is used in comparison with the stress field”. So use of stress based methods instead of strain based methods is suggested. Furthermore, especially for single objective function optimization problems, the results obtained by the principal stress method are very close to the general stress based optimality criteria method.

In this paper, the principal stress method is adopted. In each iteration,  $\theta^e$  is updated according to the angle of the principal direction at the centre of the element. For example, in the case of quadrilateral elements, if  $3 \times 3$  Gauss points are used, the principal direction obtained for the middle Gauss point can be used. If  $2 \times 2$  Gauss points are used, the average of the angles obtained for the Gauss points can be used as the updated value of  $\theta^e$  in each iteration.

## 7. Algorithm

Before explaining the algorithm, let us summarize what we have achieved so far. The structural topology optimization by the homogenization method comprises two different modules: homogenization and optimization.

In the homogenization module our aim is to establish an elastic constitutive relationship as a function of the size parameters of cellular microstructures that comprise the presumed material of each element. This is done only once and stored for all time. For the rank-layered material model, this is achieved by analytical solution of the homogenization equations. For the material model with rectangular holes, we solved the homogenization equation for a set of values of  $a$  and  $b$  and then by least square fitting we expressed the elements of the homogenized elasticity matrix as an explicit polynomial in terms of values of  $a$  and  $b$ . Therefore having the values of  $a^e$  and  $b^e$  in each element the elasticity matrix  $\mathbf{D}(a^e, b^e)$  is determined. As an easy alternative, the artificial material may be used.

It was also shown that by using frame transformation formulae, for all material models, how the effects of the orientational variables  $\theta^e$  were also considered. In summary, by use of the homogenization module  $\mathbf{D}(a^e, b^e, \theta^e)$  is obtained as an explicit function of its arguments. In the case of rank-2 materials  $a^e$  and  $b^e$  are replaced by  $\gamma^e$  and  $\mu^e$ , respectively. It is noted that calculation of the sensitivities of  $\mathbf{D}$ , which are required in the updating scheme is straightforward.

In the optimization module, considering the geometrical parameters of the presumed material model in finite elements as design variables, the total potential energy was adopted as the objective function. The volume of material was considered as the global constraint which has to be active. Forming the optimization problem, by the optimality criteria method, an updating scheme was constructed.

Now, we are in the position to construct the optimization algorithm:

1. Define the reference domain and decide upon the design and non-design domains. The design domain is the part of the domain where the microstructure is allowed to vary in the optimization process. The material of the non-design domain is fixed and is usually solid material or completely void. Choosing a suitable reference domain that allows us to introduce surface tractions and boundaries is often accomplished by intuition and engineering judgement. Here the loads, boundary conditions and the volume of material are also defined.

2. Discretize the reference domain by generating a structured or unstructured finite element mesh for analysis.
3. Initialize the design variables (i.e. the values of  $a^e$ ,  $b^e$  and  $\theta^e$ ). It should be noted that initially  $a^e$  and  $b^e$  may have different values for different elements but they have to provide a material volume close to the given volume of material. The starting values for  $\theta^e$  may be zero.
4. By means of the homogenization module, construct the elasticity matrices for each element  $\mathbf{D}(a^e, b^e, \theta^e)$ . Explicit derivatives of  $\mathbf{D}$  with respect to the design variables are also calculated.
5. Carry out a finite element analysis using the above constitutive matrices for each element and obtain displacements.
6. Evaluate the objective function and the mutual energies. Here  $E_a^e$  and  $E_b^e$  are computed according to (56) and (59).
7. Use a resizing scheme to update the design variables. Note that the scheme is affected by the value of the Lagrange multiplier of the volume constraint  $\lambda$  and consequently it has to be adjusted.
8. Check if the volume constraint is active, if it is not, update it and go back to step 7, otherwise continue.
9. Produce a new design based on the new set of updated design variables ( $a^e, b^e, \theta^e$ ) for each element  $e$ .
10. Check if the solution has converged, if it has not then use the updated design variables and go back to step 4, otherwise continue.
11. Produce a density contour plot to establish optimal topology. Other post-processing techniques (e.g. image processing) may be used to obtain a clearer image with smoother boundaries.

The above algorithm is illustrated in Fig. 3. The convergence criteria may be constructed based on the rate of variation of the objective function or the design variables. For example, the program can be terminated when, in two (or a few) successive iterations, the change in any of the design variables is not more than a given value and/or the rate of the improvement of the objective function is less than a certain value.

## 8. Examples

By employing the algorithm described in the last section, a code given the name PLATO (PLANE and PLATE topology optimization) was developed. This program is based on the optimality criteria method and allows the user to have the option to choose different material

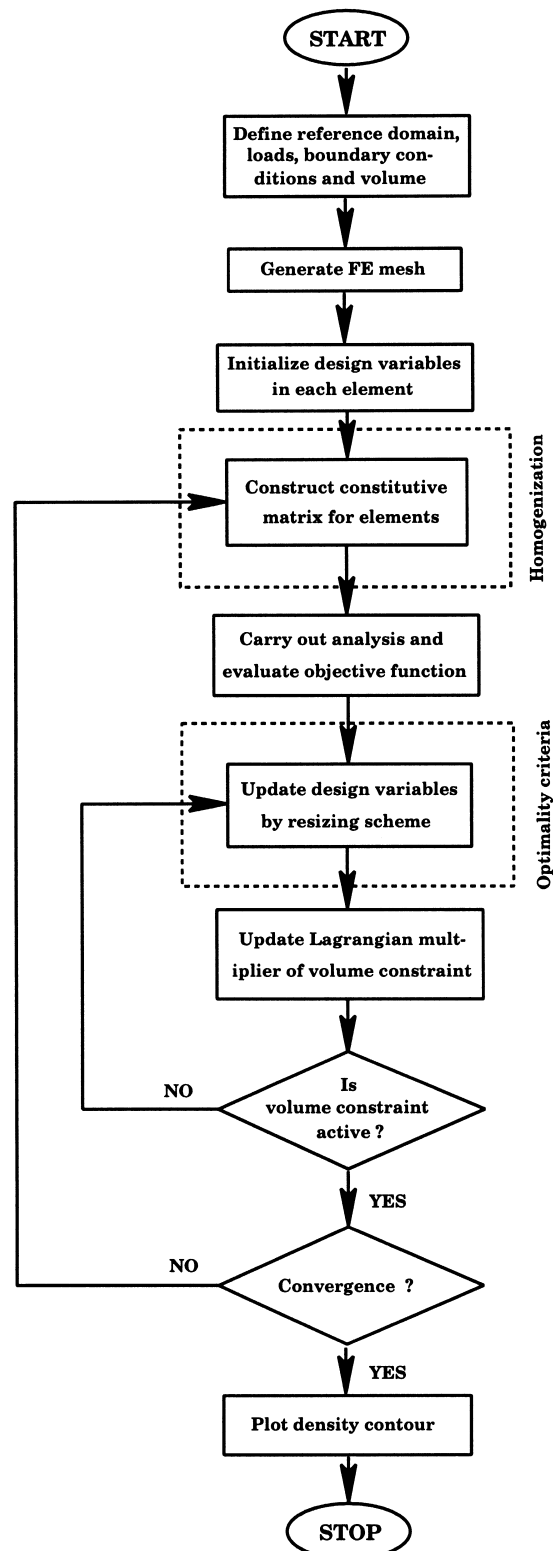


Fig. 3. Algorithm for topological structural optimization using homogenization and optimality criteria methods.

models, different element types and different resizing schemes. The following are some examples executed by PLATO.

### 8.1. Example 1

This example, which involves a clamped deep beam with a single load at the centre of the right edge, is solved as a benchmark. The problem definition is shown in the top left of Fig. 4. The Young's modulus and the Poisson's ratio are  $E = 100,000$  and  $\nu = 0.3$ , respectively. The required solid fraction  $V_{\text{solid}}/V = 20\%$  is adopted. All units are assumed to be consistent.

In this example a mesh of 8-node isoparametric elements is adopted with a  $3 \times 3$  Gauss–Legendre quadrature. For the material model, cells with rectangular voids are used. The two middle elements adjacent to the point load are considered as non-design domain. Initially the material is distributed uniformly. The final result and the iteration history are illustrated in Fig. 4. The analytical solution of this problem was discussed in Section 3.2. It was shown that the optimal layout is a two bar truss (see Fig. 2).

### 8.2. Example 2

The problem definition of a bracket with an inside hole is illustrated in Fig. 5(a). The Young's modulus and the Poisson's ratio are assumed to be 100,000 and 0.3 respectively. The radius of the hole is 2.0 and it is located in the centre of the bracket. A point load of  $P = 1000$  is applied in the top right corner. The left hand support is assumed to be fully clamped. For the volume of material  $V_{\text{solid}}/V = 30\%$  is adopted. All units are assumed to be consistent.

In this problem, the whole domain, except the hole, is considered as the design domain. The domain is discretized by an unstructured mesh of 9-node elements as illustrated in Fig. 5(b). By using the material model with rectangular holes and a complete bi-cubic least squared polynomial for data fitting the layout of Fig. 5(c) is obtained. The modified resizing scheme of Section 5.3 is employed with the resizing parameters  $\zeta = 0.006$  and  $\delta = 0.02$ .

By using the artificial material model with the penalty exponent  $\mu = 3.4$ , the layout as illustrated in Fig. 5(d) was obtained. The resizing parameters are as above.

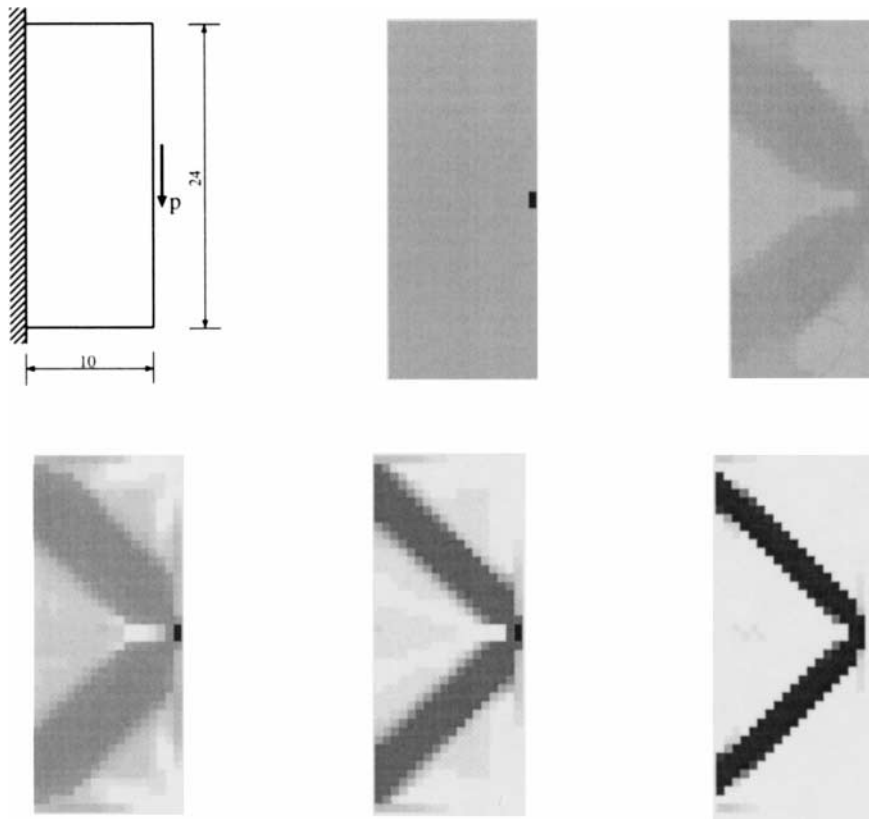


Fig. 4. Iteration history of clamped deep beam problem.

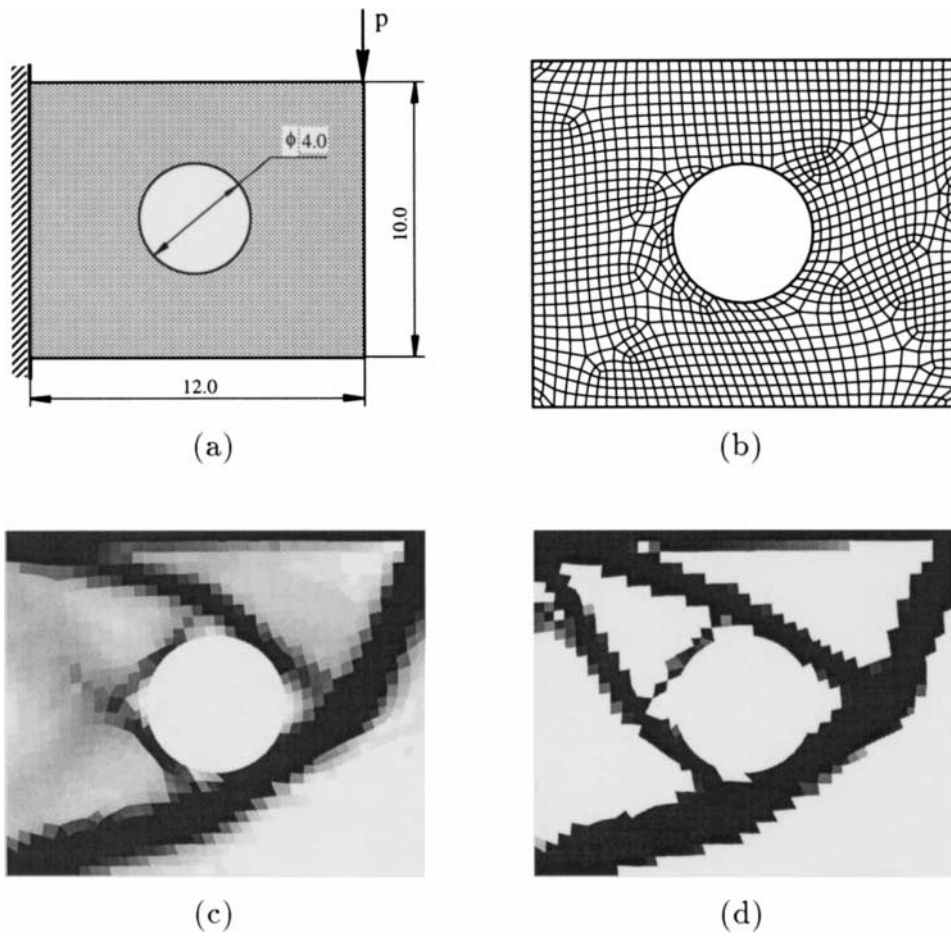


Fig. 5. (a) Problem definition; (b) finite element mesh; (c) optimal layout using the material model with rectangular voids; (d) optimal layout using the artificial material model.

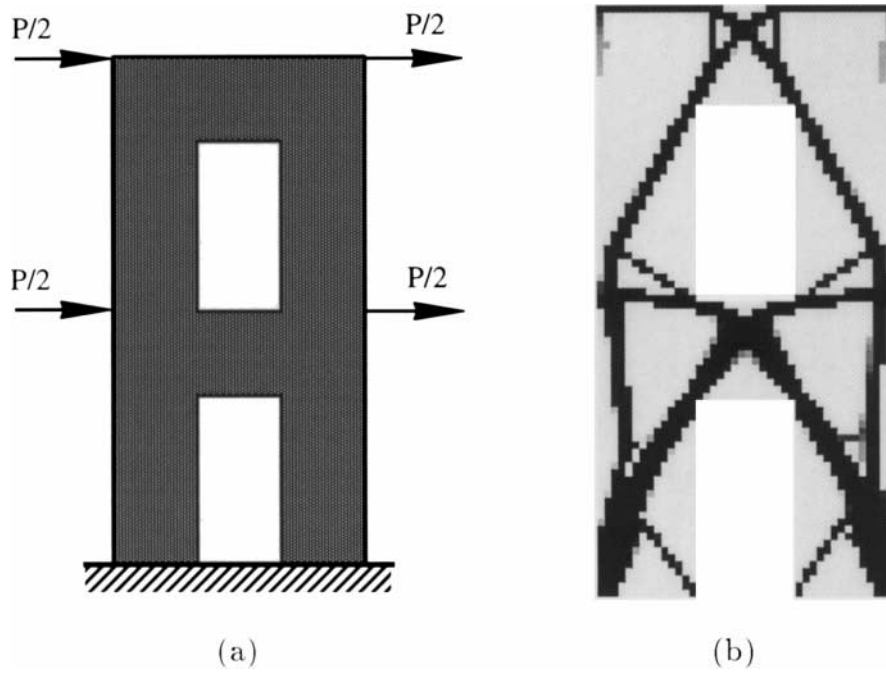


Fig. 6. (a) Geometry and loading of the shear wall problem; (b) optimal layout.

### 8.3. Example 3

The problem of finding the optimal layout of a shear wall when predefined openings exist is now considered. The problem definition is illustrated in Fig. 6(a) where horizontal point loads with intensity  $P = 1000$  are applied. The resulting optimal layout is shown in Fig. 6(b).

The artificial material model with the penalty exponent  $\mu = 3.2$  and the modified resizing scheme with  $\zeta = 0.008$  and  $\delta = 0.002$  were employed. The assumed volume fraction was taken to be  $V_{\text{solid}}/V = 30\%$ .

### 8.4. Example 4

In this example, the effect of the resizing scheme on the speed of convergence and the obtained layout is studied. For this purpose, the short cantilever beam of Fig. 7 is considered. A point load of intensity  $P = 1000$  is applied midway down the right hand side of the beam. The problem parameters are adopted as: modulus of elasticity  $E = 100,000$ , Poisson's ratio,  $\nu = 0.3$  and volume fraction  $V_{\text{solid}}/V = 40\%$ . All units are assumed to be consistent.

The artificial material model is used in this study. The move limit  $\zeta$  and the volume tolerance  $\delta$  are taken as 0.005 and 0.001, respectively. The penalty exponent  $\mu$  is chosen to be equal to 4.0.

In Section 5.2, a resizing scheme was explained. This scheme is similar to the one used by Suzuki et al [18]

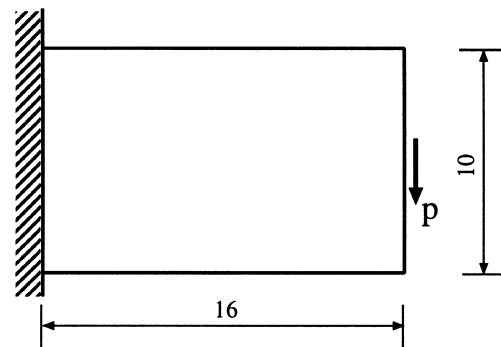


Fig. 7. Problem definition.

and Bendsøe et al [16]. When this scheme, here named Suzuki–Kikuchi's scheme, is used, after 120 iterations the strain energy is 618.0, whereas, using the suggested modified scheme of Eqs. (66) and (67) in Section 5.3 gives a value of 311.6. The iteration histories of these two experiments are shown in Fig. 8. It is observed that the modified scheme has the faster convergence. The layouts obtained after 120 iterations are shown in Fig. 9.

## 9. Conclusions and Final Remarks

In this final part of a three paper review, the mathematical model for the topological structural optimization has been constructed and derivation of the related optimality criteria has been explained. A modi-

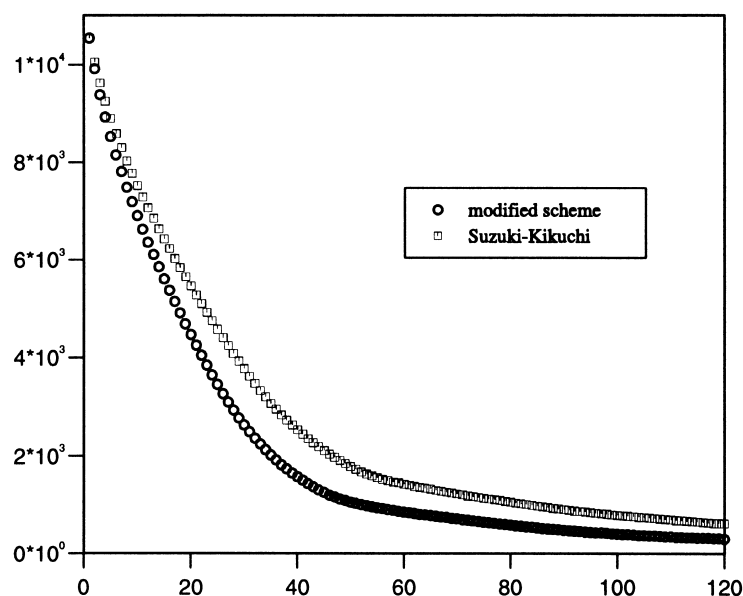


Fig. 8. Iteration history using two different resizing schemes.



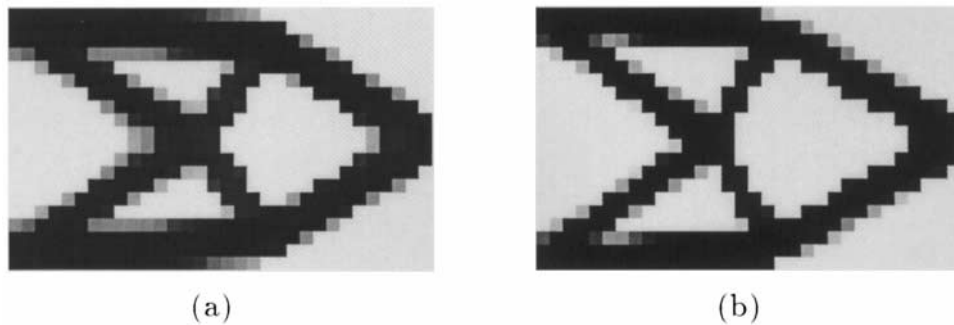


Fig. 9. Layout obtained after 120 iterations using artificial material model and two different schemes: (a) Susuki-Kikuchi's scheme; and (b) modified scheme.

fied resizing scheme has been suggested. Finally, some illustrative examples were provided.

It is appropriate to emphasize that in this review, several topics have been omitted due to space constraints. Only topology optimization of two-dimensional continuum problems subjected to a single load case have been considered. Furthermore, only compliance minimization has been presented. However, these omissions are not limitations of the method itself. Multiple load cases can be catered for using the sum of suitably weighted compliances for each load case. Objective functions other than compliance can be adopted. For example, it is possible to maximize the fundamental frequency of a structure. Constraints other than volume constraints may be included. The concepts considered in this review may be extended to shells and three dimensional models. Indeed, other forms of physical behaviour can be incorporated. This is a rich area for investigation and one very interesting avenue of research is the optimal design of material microstructures which exhibit unusual behaviour which involve apparent constitutive relationships with negative Poisson's ratios and negative coefficients of thermal expansion thus opening up the possibility of designing "made-to-measure" materials [25].

Other forms of topology optimization exist; see for example, the text on evolutionary (hard-kill) strategies by Xie and Stevens [26]. For a more detailed account of the subjects outlined in this review, we recommend the texts of Bendsøe [27] and Rozvany [5] and review by Rozvany et al [6]. Finally, we would also draw attention to our new text on these subjects which includes some software for both homogenization and topology optimization.

#### Acknowledgements

The moral and financial support of Behim Dezh Co. and the University of Shahroud (Iran) is gratefully acknowledged.

#### References

- [1] Haftka RT, Gürdal Z. Elements of structural optimization. 3rd ed. Kluwer, Dordrecht, 1992.
- [2] Kirsch U. Structural optimization. Springer, Berlin, 1993.
- [3] Rozvany GIN, Zhou M. The coc algorithm, part i: cross section optimization or sizing. *Comp Meth Appl Mech* 1991;89:281–308.
- [4] Michell AGM. The limits of economy of material in frame-structures. *Phil Mag* 1904;8:305–16.
- [5] Rozvany GN. Structural design via optimality criteria. Kluwer, Dordrecht, 1989.
- [6] Rozvany GN, Bendsøe MP, Kirsh U. Layout optimization of structures. *Appl Mech Rev* 1995;48(2):41–119.
- [7] Rozvany GIN, Zhou M. Optimality criteria methods for large discretized systems. In: Adeli H, editor. *Advances in design optimization*. Chapman & Hall, London, 1994. p. 41–108.
- [8] Rozvany GIN, Zhou M, Sigmund O. Optimization of topology. In: Adeli H., editor. *Advances in design optimization*. Chapman & Hall, London, 1994. p. 340–399.
- [9] Zhou M, Rozvany GIN. Deoc: an optimality criteria method for large systems, part i: theory. *Struct Optimiz* 1992;5:12–25.
- [10] Rozvany GIN, editor. *Shape and layout optimization of structural systems and optimality criteria methods*. Springer, CISM, Udine, 1992.
- [11] Kuhn HW, Tucker AW. Nonlinear programming. In: Neyman J, editor. *Proceedings of the second Berkeley symposium on mathematical statistics and probability*, University of California Press, Berkeley, California, 1951. p. 481–492.
- [12] Wismer DA, Chattergy R. *Introduction to nonlinear optimization*. North Holland, New York, 1979.
- [13] Olhoff N, Taylor JE. On structural optimization. *J Appl Mech* 1983;50:1139–51.
- [14] Reddy JN, Rasmussen ML. *Advanced engineering analysis*. Wiley, New York, 1982.
- [15] Reddy JN. *Applied functional analysis and variational methods in engineering*. McGraw-Hill, New York, 1986.
- [16] Bendsøe MP, Díaz AR, Kikuchi N. Topology and generalized layout optimization of elastic structures. In:

- Bendsøe MP, Mota Soares CA, editors. *Topology design of structures*. Kluwer, Dordrechts, 1993. p. 159–205.
- [17] Washizu K. *Variational methods in elasticity and plasticity*. 3rd ed. Pergamon Press, Oxford, 1982.
- [18] Suzuki K, Kikuchi N. A homogenization method for shape and topology optimization. *Comp Meth Appl Mech Engng* 1991;93:291–318.
- [19] Berke L, Khot NS. Use of optimality criteria for large scale systems. AGARD LS-70, 1974.
- [20] Chung TJ. *Continuum mechanics*. Prentice-Hall, London, 1988.
- [21] Pedersen P. On optimal orientation of orthotropic materials. *Struct Optimiz* 1989;1:101–6.
- [22] Cheng HC, Kikuchi N, Ma ZA. An improved approach for determining the optimal orientation of orthotropic material. *Struct Optimiz* 1994;8:101–12.
- [23] Bendsøe MP. Optimal shape design as a material distribution problem. *Struct Optimiz* 1989;1:193–202.
- [24] Díaz AR, Bendsøe MP. Shape optimization of multipurpose structures by a homogenization method. *Struct Optimiz* 1992;4:17–22.
- [25] Sigmund O. Materials with prescribed constitutive parameters: an inverse homogenization problem, Technical Report 470. The Technical University of Denmark, 1993.
- [26] Xie YM, Steven GP. *Evolutionary structural optimization*. Springer, Berlin, 1997.
- [27] Bendsøe MP. *Optimization of structural topology, shape, and material*. Springer, Berlin, 1995.